

https://doi.org/10.1070/QEL16530

Analysis of the influence of geometrical dimensions and external magnetic field on optical properties of InGaAs/GaAs quantum-dot slow light devices

B. Choupanzadeh, H. Kaatuzian, R. Kohandani

Abstract. **The effect of the size of quantum dots (QDs) and an external magnetic field on InGaAs/GaAs QD slow light devices based on coherent population oscillations (CPOs) is simulated. Physical parameters of QDs, such as radius and height, are varied around their central mean values, which are assumed to be 8 and 5 nm, respectively. An attempt is made to obtain much better optical characteristics by applying a strong external magnetic field. The methods used to improve the optical properties of a QD slow light device, such as the slow down factor (SDF), bandwidth and exciton binding energy, are discussed. It is shown that a QD slow light device makes it possible to shift the centre frequency in a range of 5 THz and to achieve a slow down factor of 5000.**

Keywords: *quantum dots, excitonic population oscillations, slow light, shift of the centre frequency, slow down factor.*

1. Introduction

Recently, slow light has attracted great attention as a way to control the speed of light [1]. Slow light plays an important role in photonic devices. One of the usages of slow light is the ability to store a light signal in optical buffers [2] in order to make delay lines [3]. Other applications of slow light include data packet synchronisation, optical gates and bit level synchronisation [4–6]. Rapid alterations of the refractive index in a resonant frequency of the material [7] are used to reduce the speed of light or to achieve the slow light. There are different methods and techniques to slow down the speed of light: electromagnetically induced transparency (EIT), coherent population oscillation (CPO), stimulated Raman scattering (SRS) and stimulated Brillouin scattering (SBS) [8, 9]. In particular, the EIT method has been implemented in warm and cold gases with three level atoms and experts could reach a small group velocity of about 8 m s^{-1} [7].

Controlling the speed of light is of great importance in solid state semiconductors because these materials have a potential to be used in photonic devices such as optical memories and optical quantum processors [10]. In order to reduce the speed of light in semiconductors, several methods have been proposed. In recent years, coherent population oscillation (CPO) has been considered by many researchers. This method has some benefits such as a vast range of working temperatures, capability to adjust the buffer parameters and greater adaptability with optical circuits [11, 12].

The CPO is used in semiconductor quantum wells (QWs) and quantum dot (QDs) in a large range of working temperatures [11, 12]. In these structures, CPO uses the excitons lifetime to control the speed of light. This method ensures a steep slope in the real part of the refractive index and reduces the group velocity. Slow light in semiconductor QWs and QDs has been widely investigated both theoretically and experimentally [13–18]. The CPO method in QDs is similar to that in QWs. But there is a three-dimensional (3D) confinement of the carriers in QDs. This 3D confinement will increase the probability of slow light occurrence at room temperature [11, 12].

In this paper, we report several theoretical techniques to modify optical properties of a quantum dot slow light device based on CPO. In these methods, an external magnetic field is applied to a QD structure with variable dimensions, which allows one to control optical characteristics of a QD slow light device, such as slow down factor and centre frequency.

2. Theory

2.1. Structure of a semiconductor QD slow light device based on CPO

Slow light is an optical signal propagating at a very small group velocity. The group velocity of light in a dispersive medium is obtained from the equation [7]:

$$v_{\mathrm{gr}} = \frac{c}{n(\omega) + \omega \partial n(\omega)/\partial \omega}, \tag{1}$$

where ω is the frequency, c is speed of light in vacuum and $n(\omega)$ is the refractive index [7]. In a two-level system, if the difference between the frequency of the signal and pump (detuning) are applied to the system is within the reverse lifetime of the carriers, there will be a significant population oscillation [1]. These population oscillations can make a dip in the absorption curve of the system and cause a drastic change in the real part of the refractive index, which eventually sharply reduces the group velocity. This two-level system in a semiconductor could be a conduction band and heavy-hole exciton band. The dynamic equations of the density matrix elements for a QD system in the two-level approximation can be found elsewhere [19].

The time-dependent Rabi frequencies $\Omega_{1\uparrow(2\downarrow)}$ are expressed through the pump and signal parameters as follows:

B. Choupanzadeh, H. Kaatuzian, R. Kohandani Photonics Research Lab, Electrical Engineering Department, Amirkabir University of Technology, Tehran, Iran; e-mail: hsnkato@aut.ac.ir

Received 5 October 2017; revision received 6 January 2018
Kvantovaya Elektronika **48** (6) 582–588 (2018)
Submitted in English

$$\Omega_{1\uparrow}(t) = \Omega_{s,\uparrow 1}\exp(-j\omega_p t) + \Omega_{p,\uparrow 1}\exp(-j\omega_p t), \quad (2)$$

$$\Omega_{2\downarrow}(t) = \Omega_{s,2\downarrow}\exp(-j\omega_p t) + \Omega_{p,2\downarrow}\exp(-j\omega_p t), \quad (3)$$

$$|\Omega_{p,\uparrow 1}| = |\Omega_{p,\downarrow 1}| = \frac{|I_{ch} e r_{ch} E_p|}{2\sqrt{2}\,h}, \quad (4)$$

$$|\Omega_{s,\uparrow 1}| = |\Omega_{s,\downarrow 1}| = \frac{|I_{ch} e r_{ch} E_s|}{2\sqrt{2}\,h}, \quad (5)$$

where $p_{1\uparrow(2\downarrow)}$ is the medium polarisation induced by the pump and the signal; I_{ch} is the overlap of the wave functions of the electron and hole in the variational wave function of the exciton; er_{ch} is the interband dipole moment of the transition; E_s is the optical field of the signal; and E_p is the optical field of the pump.

After solving the mentioned dynamic equations, the device's permeability tensor can be obtained as follows [19]:

$$\varepsilon_s(\omega_s) = \varepsilon_{bgd} + n_d \pi \int f(r) r^2 (\chi_x(\omega_s, r))\,dr. \quad (6)$$

Here, $n_d = N_d/A$ is the number of QDs per unit area; χ_x is the susceptibility; ω_s is the signal frequency; $f(r)$ is simulated by the Gaussina distribution and determined by the expression [19]

$$f(r) = \frac{1}{\sigma_s\sqrt{2\pi}}\exp\left[\frac{(r-\bar{r})^2}{2\sigma_s^2}\right]; \quad (7)$$

$\bar{r}$ is the mean value of the QD radius; r is the QD radius; and σ_s is the standard deviation of the QD radius. A detailed description of calculations is available in Ref. [19]

The refractive index, absorption coefficient and slow down factor in semiconductor structures are defined as follows [19]:

$$n_s(\omega_s) = \sqrt{\varepsilon_{bgd} + \chi_x(\omega_s)}, \quad (8)$$

$$A_s(\omega_s) = 2\,\mathrm{Im}(n_s(\omega_s)), \quad (9)$$

$$R_s(\omega_s) = \mathrm{Re}(n_s(\omega_s)) + \omega_s \frac{\partial\,\mathrm{Re}(n_s(\omega_s))}{\partial\omega_s}. \quad (10)$$

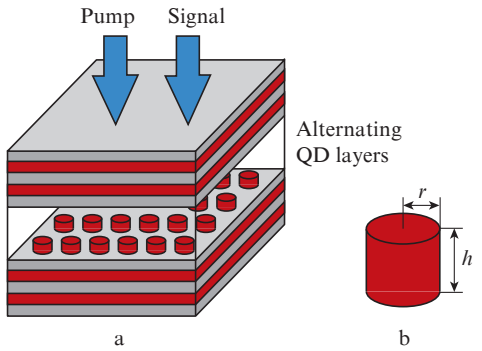

Figure 1. (a) Pump–probe scheme for excitation of coherent population oscillations in an ensemble of QDs and (b) the geometry of a QD. The QD is modelled as a cylinder with height h and radius r [19].

Figure 1a shows the schematic of a CPO-based quantum dot system for slowing light. In this QD slow light device, QDs are identical and uniformly distributed in the plane of the wetting layer. The geometry of quantum dots is shown in Fig. 1b. In this quantum dot, the signal and the pump propagate in the same direction [19].

Consider a CPO-based $In_{0.25}Ga_{0.75}As/GaAs$ QD slow light device similar to that in Fig. 1. According to Ref. [19], the QD radius is equal to 8 nm, the height is 5 nm and the QD density amounts to 10^{14} m^{-2}. In this device, the pump power is equal to 1 kW cm^{-2}. At a mean QD radius of 8 nm, the exciton energy is 1.294 eV (at λ = 958 nm) [19]. Using equations (2)–(5) and above parameters, we could simulate the slow light device. Figure 2 illustrates the absorption, real part of the refractive index and slow down factor of a QD slow light device presented in [19] as a function of detuning frequency.

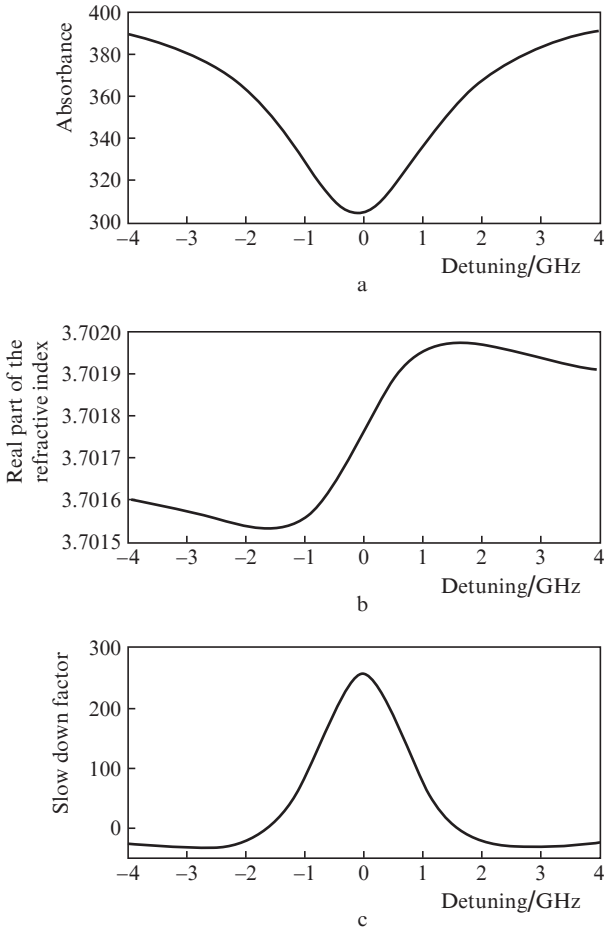

Figure 2. (a) Absorbance, (b) real part of the refractive index, and (c) slow down factor plotted as functions of detuning between the frequencies of the signal and the pump due to excitonic population oscillations in InGaAs/GaAs quantum dots described in [19, 20].

As it can be seen from Fig. 2b, the steepest slope (positive slope) of the real part of the refractive index occurs at the zero detuning frequency. Thus, it can be expected that the maximum SDF value occurs in this frequency and the accuracy of this guess can be seen in Fig. 2c. Also, it can be seen from Fig. 2c that the maximum SDF is 250; one of our aims in this research is to enhance the SDF value [19, 20].

2.2. Variation of exciton binding energy due to QD radius changes

Binding energy of excitons in a QD structure can be determined as a function of the dot radius [21]:

$$E_B = \frac{h^2\pi^2}{2r^2}\left[\frac{1}{m_e} + \frac{1}{m_h}\right] - \frac{1.786e^2}{\varepsilon r} - 0.248E_R, \quad (11)$$

where m_e and m_h are the effective masses of the electron and the hole, respectively; ε is the dielectric constant; and E_R is bulk exciton binding energy. Figure 3 shows the exciton binding energy as a function of the QD radius. Full details of calculation can be found in [21, 22].

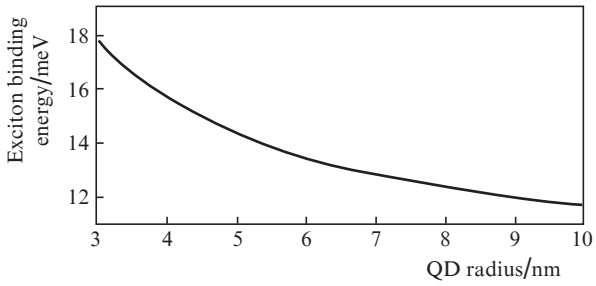

Figure 3. Exciton binding energy as a function of the QD radius [22].

The exciton energy in a semiconductor QD slow light device can be defined through the exciton binding energy and band gap energy. This relationship can be expressed in the form [16]:

$$E_{ex} = E_{\text{band gap}} - E_{\text{binding energy}}. \quad (12)$$

The centre frequency of a semiconductor slow light device based on excitonic population oscillations can be determined with the exciton energy [16].

2.3. Effects of an applied magnetic field on QD structures

In this section, we investigate the impact of applying a magnetic field on a QD slow light device. According to paper [23], after the magnetic field is applied, the exciton energy will change. The relationship between the applied magnetic field and the exciton energy shift is found from the expression [23]:

$$\Delta E = \frac{1}{2}h\sqrt{w_c^2 + 4w_p^2}. \quad (13)$$

Here, $w_c = eB/\mu$ is the electron cyclotron frequency and $2hw_p$ is the in-plane QD confinement energy [23]. In the QD structures, the confinement energy depends on the QD geometric sizes. Figure 4 shows the confinement energy as a function of QD radius and QD height, respectively [24, 25].

Figure 5 shows the relationship between the applied magnetic field and the exciton energy. One can see that it is close to a straight proportional dependence. This means that by increasing the magnetic field, the exciton energy will also increase, because the magnetic field associated with the cyclotron energy prevails over the coulomb energy [22].

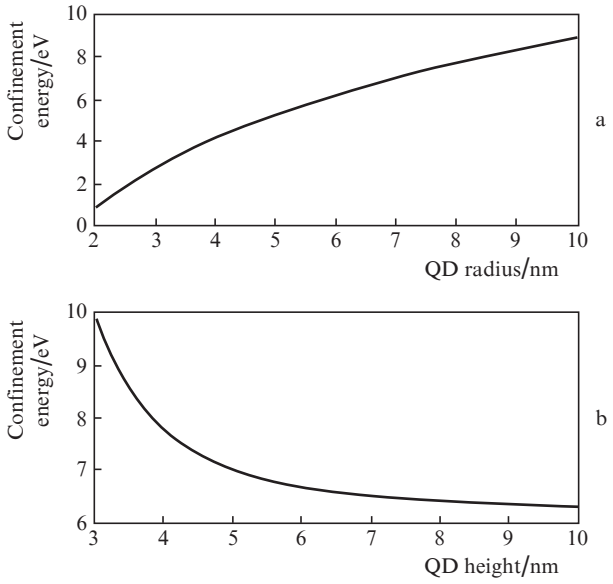

Figure 4. Confinement energy as a function of (a) radius and (b) height [24, 25].

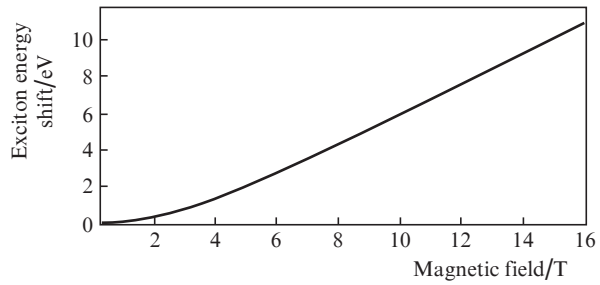

Figure 5. Exciton energy shift as a function of magnetic field [23].

As was mentioned in Section 2.2, the centre frequency of the QD slow light device is determined by the exciton energy. Consequently, by applying an external magnetic field, the centre frequency of the slow light device will change.

2.4. Effect of QD height variation on the exciton binding energy

The exciton binding energy is dependent on the geometric size of the QD. The relation between the QD radius and the exciton binding energy is determined in Section 2.2. In this section, the relation between the exciton binding energy and the QD height is investigated. Figure 6 shows the dependence

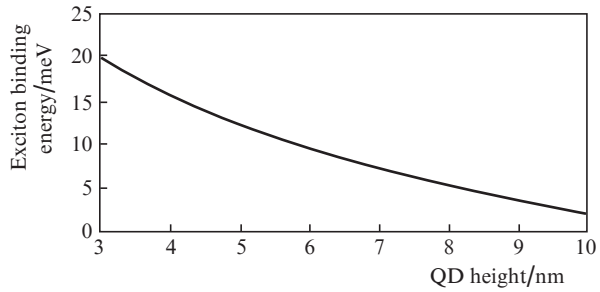

Figure 6. Exciton binding energy as a function of QD height [26].

of the exciton binding energy on the QD height (more details can be found in Ref. [26]). One can see that by decreasing the QD height, the exciton binding energy will increase. Thus, by changing the QD height, we can eventually shift the centre frequency of the slow light device.

3. Results and discussion

3.1. Effect of QD radius alterations on slow light device properties

According to Section 2.2, QD radius alterations will affect the exciton energy and finally leads to a shift of the centre frequency of the slow light devices. Figure 7 shows the real part of the refractive index and slow down factor of the QD slow light device for three different QD radii. One can see that by changing the QD radius, both the exciton energy and the slow down factor will be affected. When the QD radius increases, the binding energy decreases. Then according to equation (12), both the exciton energy and the centre frequency increase. Moreover, by increasing the QD radius, the slow down factor decreases.

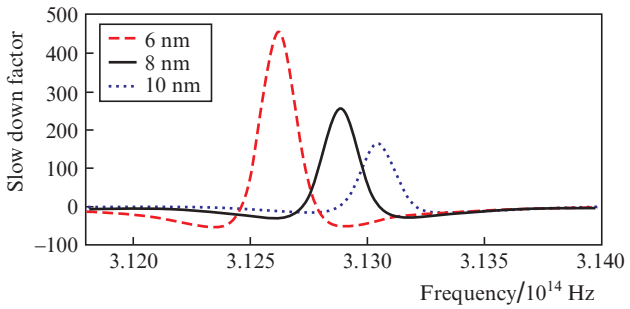

Figure 7. Slow down factor of the slow light device for three different QD radii as a function of frequency. The solid line is the results from Ref. [19].

Figure 8 can be useful for a better understanding of variations of the SDF value and the amount of centre frequency shift. 3D curves of the refractive index in Fig. 8 are plotted for simultaneous changes in radius and frequency. When the radius decreases, the slope of the real part of the refractive index increases, and consequently, the SDF value will increase whereas the centre frequency will shift to the lower frequencies.

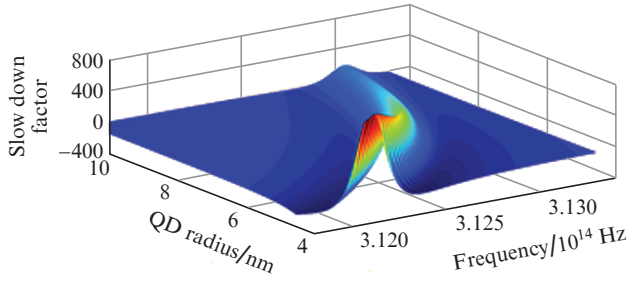

Figure 8. Slow down factor of the slow light device as function of QD radius and frequency.

3.2. Effect of the applied magnetic field on optical characteristics of a QD slow light device

Applying an external magnetic field enhances the exciton energy. A vriation of the exciton energy as a function of the applied magnetic field is shown in Fig. 9. After applying three different values of magnetic fields, the slope of the SDF value in Fig. 9 has not changed, which means that applying an external magnetic field has no effect on the group refractive index and SDF of the slow light device. Nevertheless, as an external magnetic field is applied to the device, the exciton energy increases and as expected, the centre frequency of the device shifts to higher frequencies. This approach can be used for post-fabrication tuning of the slow light device.

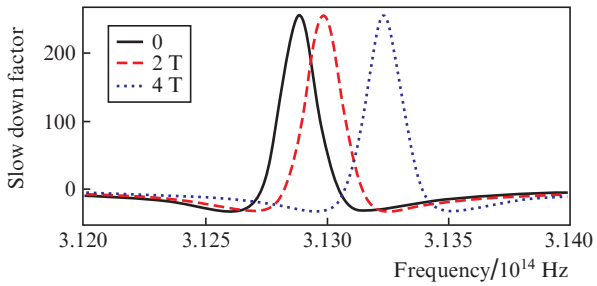

Figure 9. Slow down factor of the slow light device for three different values of the applied magnetic field. The solid line is the results from Ref. [19].

3.3. Effect of QD height on properties of the slow light device

Figure 10 shows the dependence of the SDF on the frequency for three different QD heights. According to this figure, after decreasing the QD height, the slope of the real part of the refractive index increases and consequently, the slow down factor increases. Furthermore, by decreasing the QD height, the exciton energy reduces and the centre frequency of the device reaches lower values.

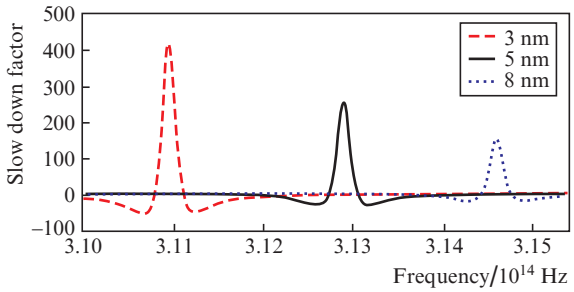

Figure 10. Slow down factor of the slow light device for three different QD heights. The solid curve is the results from Ref. [19].

Figure 11 can be useful for a better understanding of the conclusion about the behaviour of SDF and centre frequency shifts. 3D curves of the slow down factor in Fig. 11 are plotted for simultaneous changes in height and frequency. The dependence on the height shows that when the height decreases, the slope of the real part of the refractive index increases, and consequently, the SDF value will increase, whereas the centre

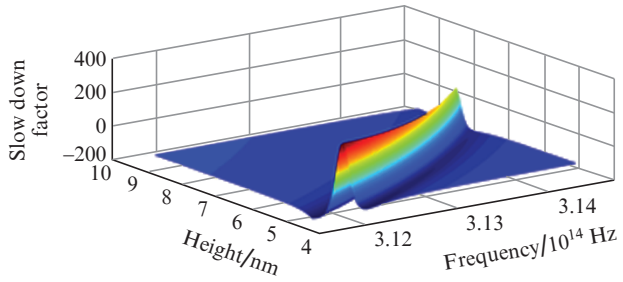

Figure 11. Variation of the slow down factor of the device as a function of radius and frequency.

frequency will shift to the lower frequencies. In contrast, by enhancing the QD height, the SDF value decreases and the centre frequency reaches higher frequencies. Thus, changes in the QD radius and height affect the slow light device in almost the same manner.

3.4. Effect of the QD radius under an applied magnetic field

Figure 12 shows the maximum SDF value as a function of both the QD radius and the applied magnetic field. One can see that applying an external magnetic field has no effect on the maximum SDF value. Thus the SDF value is independent of the amount of the applied magnetic field.

Figure 13 shows the 3D curve of the central frequency shift as a function of QD radius and applied magnetic field.

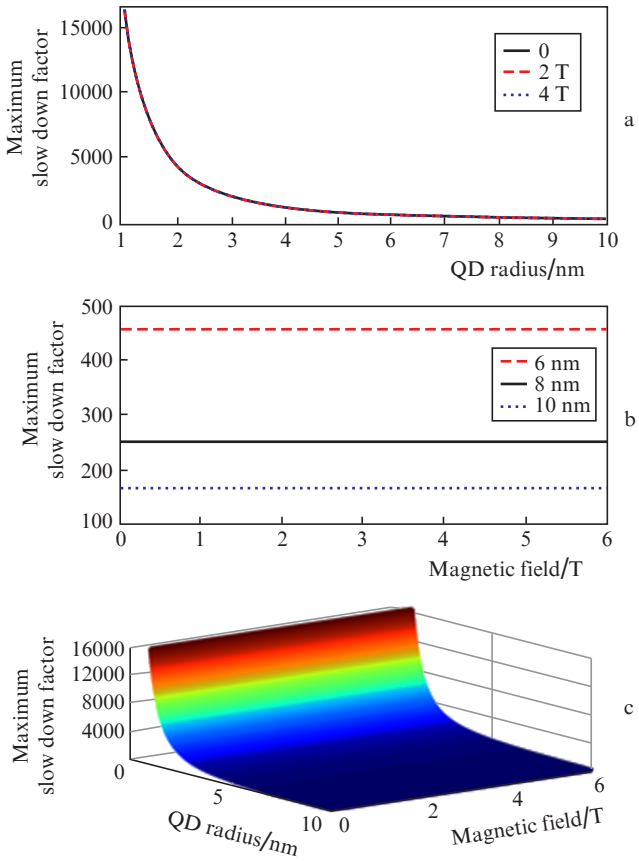

Figure 12. Maximum value of the slow down factor vs. (a) QD radius for magnetic fields of 0, 2 and 4 T, vs. (b) magnetic field for QD radii of 5, 8 and 10 nm, and vs. (c) radius and magnetic field changing simultaneously.

According to this figure and theories mentioned in the previous sections, before applying a magnetic field to the device, the centre frequency shift for a QD radius of 8 nm is zero. When the QD radius is more than 8 nm, the centre frequency shift reaches positive values and when the QD radius is less than 8 nm, the centre frequency shift reaches negative values. By applying a magnetic field and changing the QD radius simultaneously, the frequency shift would be the result of both QD radius variations and applied magnetic fields. The effect of QD radius alterations on the frequency shift can be explained using equation (13). According to this equation, by applying an external magnetic field to the device, the exciton energy will increase and lead to a shift of the centre frequency to higher values. In addition, by varying the amount of the applied magnetic field and the QD radius simultaneously, two phenomena will determine the amount of the energy shift [see Eqn (13)]. Firstly, by altering the applied magnetic field, the variable w_c will change. Secondly, by changing the QD radius under an applied magnetic field, the variable w_p, which presents the amount of the confinement energy in QDs, will vary (see Fig. 4a). Thus, the centre frequency shift under an applied the magnetic field varies due to both variations of magnetic fields and confinement energy (which is dependent on the QD radius). These results can be useful for tuning the optical properties of the device before and after fabrication.

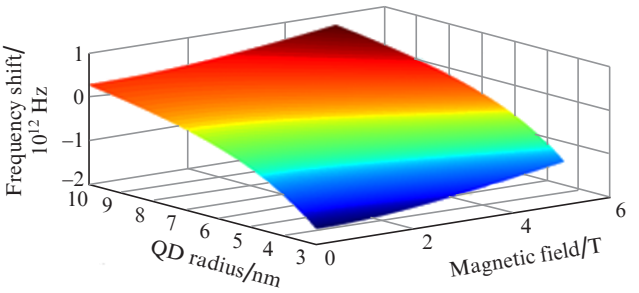

Figure 13. Frequency shift as a function of radius and magnetic field.

3.5. Effect of the QD height under an applied external magnetic field

In this section, we investigate the effect of changing the QD height under an applied magnetic field. Figure 14 shows the maximum SDF value as a function of both QD height and applied magnetic field. One can see that by increasing the height of QDs, the maximum SDF value is reduced. In accordance with the results in Sections 3.2 and 3.4, the data of Fig. 14 demonstrate that the magnetic field has no effect on the maximum SDF.

Figure 15 shows the frequency shift for the slow light device as a function of both QD height and applied magnetic field. In the absence of the magnetic field, the change in the QD height leads to a change in the centre frequency. The frequency shift will reach positive values for QD heights more than 5 nm and negative values for QD heights less than 5 nm. After applying magnetic field to the device, the centre frequency shift would be the result of both QD height variations and applied magnetic fields. The QD height variations have already been discussed above and the effect of applied magnetic field can be described using equation (13). According to this equation, applying the magnetic field will increase the exciton energy and therefore the centre frequency will shift to

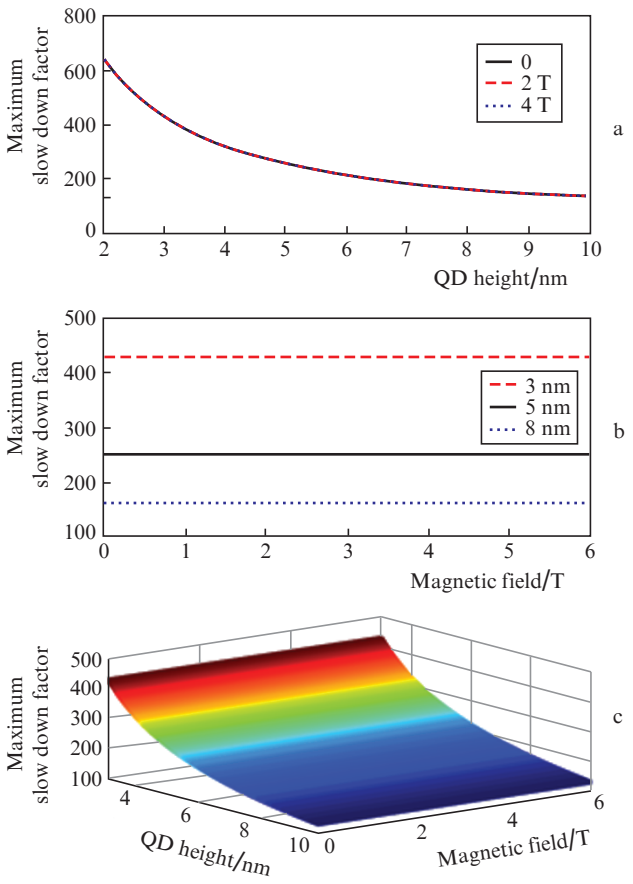

Figure 14. Maximum value of the slow down factor vs. (a) QD height for magnetic fields of 0, 2 and 4 T, vs. (b) magnetic field for QD heights of 3, 5 and 8 nm, and vs. (c) QD height and magnetic field changing simultaneously.

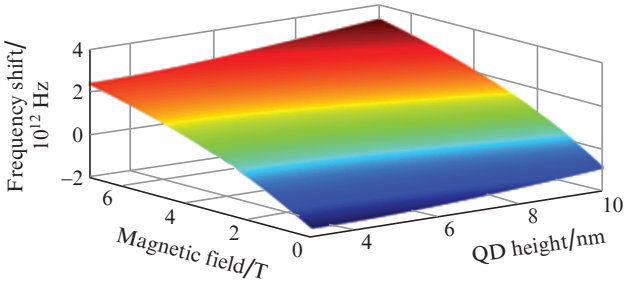

Figure 15. Frequency shift as a function of height and magnetic field.

higher values. Furthermore, by altering the applied magnetic field and QD height simultaneously, two phenomena will happen. Firstly, the parameter w_c in equation (13) will change due to alteration of the applied magnetic fields and cause the variation of centre frequency shift. Secondly, the parameter w_p will change due to both the magnetic field and the QD height. The dependence of the confinement energy on the QD height has already been illustrated in the Fig. 4b.

3.6. Effect of simultaneous changes of the QD radius and height on the QD slow light device

Figure 16 illustrates variations of the maximum SDF value as a function of both QD radius and height. In this approach, we managed to reach a high slow down factor of 5000.

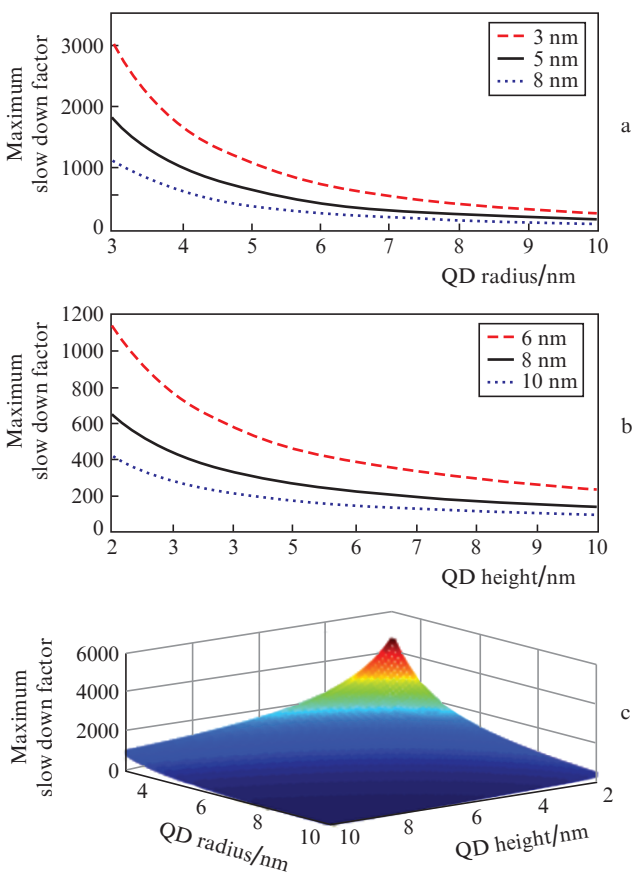

Figure 16. Maximum value of the slow down factor vs. (a) QD radius for QD heights of 3, 5 and 8 nmT, vs. (b) QD height for QD radii of 6, 8 and 10 nm, and vs. (c) QD radius and height changing simultaneously.

By changing the QD dimensions, not only SDF value will be changed but also the centre frequency of the QD slow light device will be shifted. Figure 17 shows the frequency shift for the slow light device as a function of both QD radius and height.

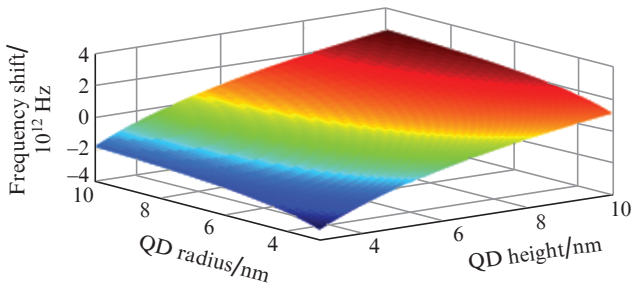

Figure 17. Centre frequency shift as a function of height and radius.

4. Conclusions

In this paper, we have investigated an InGaAs/GaAs semiconductor QD slow light device based on excitonic population oscillations under an applied magnetic field. Also the simulation results are presented for the quantum dots of different radii and heights. Based on obtained results, by altering the physical dimensions of the quantum dots under a strong

external magnetic field, significant properties of the slow light device, such as central frequency and slow down factor, could be changed. By increasing QD radius or height, the centre frequency shifts to higher frequencies and the slow down factor reaches lower values. Using this approach, we have managed to reach a high slow down factor of 5000. Moreover, applying an external magnetic field shifts the centre frequency to higher frequencies but has no effects on the slow down factor. Furthermore, the frequency shift can be maximised by applying a strong magnetic field to the device optimised with respect to the QD radius and height. In this case, the centre frequency of the QD slow light device can be shifted in a range of 5 THz. These results can be used in optical nonlinearity enhancements, all-optical signal processing applications, and optical communications [16].

References

1. Chang S.W., Chuang S.L., Ku P.C., Chang-Hasnian C.J., Palinginis P., Wang H. *Phys. Rev. B*, **70**, 235333 (2004).
2. Chang-Hasnian C.J. *J. Lightwave Technol*., **24** (12), 4642 (2006).
3. Chang Shu-Wei, Kondratko P.K., Su H. *IEEE J. Quantum Electron.*, **43** (2), 249 (2007).
4. Parra E., Lowell J.R. *Opt. Photon. News*, **18**, 40 (2007).
5. Kash M.M., Sautenkov V.A., Zibrov A.S., Hollberg L., Welch G.R., Lukin M.D., Rostovtsev Y., Fry E.S., Scully M.O. *Phys. Rev. Lett*., **82**, 5229 (1999).
6. Pesala B., Chen Z.Y., Uskov A.V., Chang-Hasnain C. *Opt. Express*, **14**, 12968 (2006).
7. Gauthier D.J., Gaeta A.L., Boyd R.W. *Photon. Spectra*, 44 (Mar. 2006).
8. Kaatuzian H. *Photonics* (AKU Press, 2017) Vol. 2.
9. Bigelow M.S., Lepeshkin N., Boyd R.W. *Science*, **301** (5630), 200 (2003).
10. Ma S.M., Xu H., Ham B.S. *Opt. Soc. Am.*, **17** (17), 2850 (2009).
11. Sun D., Ku P.C. *J. Lightwave Technol*., **26**, 3811 (2008).
12. Chang-Hasnian C.J., Ku P.C., Kim J., Chuang S.L. *Proc. IEEE*, **91**, 1884 (2003).
13. Kaatuzian H., Kohandani R. *Proc. 23rd Iranian Conference on Electrical Engineering* (Tehran, 2015) pp 1385–1388.
14. Kohandani R., Kaatuzian H. *Quantum Electron*., **45** (1), 89 (2015) [*Kvantovaya Elektron*., **45** (1), 89 (2015)].
15. Kaatuzian H., Kojori H.S., Zandi A., Kohandani R. *Opt. Photon. J*., **3** (2), 298 (2013).
16. Kohandani R., Zandi A., Kaatuzian H. *Appl. Opt*., **53**, 1228 (2014).
17. Mork J., Kjaer R., van der Poel M., Yvind K. *Opt. Express*, **13** (20), 8136 (2005).
18. Su H., Chuang S.L. *Opt. Lett*., **31** (2), 271 (2006).
19. Chang S.-W., Chuang S.L. *Phys. Rev. B*, **72**, 235330 (2005).
20. Choupanzadeh B., Kaatuzian H., Kohandani R., Abdolhosseini S. *Opt. Photon. J.*, **6**, 114 (2016).
21. Thao T.T., Viet N.A. *Commun. Phys*., **14** (2), 95 (2004).
22. Bayer M., Walck S.N., Reinecke T.L., Forchel A. *Phys. Rev. B*, **57**, 6584 (1998).
23. Tyan S.L., Lin Y.G., Tsai F.Y., Lee C.P., Shields P.A., Nicholas R.J. *InGaAs/GaAs Quantum Wells and Quantum Dots on (111)B Orientation* (Elsevier Sci. Ltd, 2001) Vol. 117, p. 649.
24. Chukwuocha E.O., Onyeaju M.C., Harry T.S.T. *World J. Condens. Matter Phys*., **2**, 96 (2012).
25. Perinetti U. *Optical Properties of Semiconductor Quantum Dots* (Delft–Leiden, Casimir PhD Series, 2011).
26. Holma M., Pistol M.E. *Appl. Opt.*, **92**, 15 (2002).